Contents lists available at SciOpen

Food Science and Human Wellness

journal homepage: https://www.sciopen.com/journal/2097-0765

China Food Publishing Co.

# Cyanidin 3-*O*-*β*-galactoside from black chokeberry exerts neuroprotective effects in mice fed with high-fat/high-sugar diet through regulating glucose metabolism

Zhuoyan Fan[a,1], Xiaoyu Liu[a,1], Wentao Gao[a], Lei Zhang[a], Xinquan Yang[b,*], Jingming Li[a,*]

[a] College of Food Science and Nutritional Engineering, China Agricultural University, Beijing 100083, China
[b] Clinical Laboratory Center of Medicine, Zhongshan City People's Hospital, Zhongshan 528403, China

ARTICLE INFO

*Article history:*
Received 17 March 2024
Received in revised form 31 March 2024
Accepted 11 April 2024

*Keywords:*
Cyanidin 3-*O*-*β*-galactoside
Glucose metabolism
Neuroprotection
Cognitive impairment
Energy supply

ABSTRACT

Unhealthy diets are associated with various diseases that can disrupt brain energy metabolism, which significantly increased the risk of cognitive impairment and chronic neurodegenerative diseases. Early intervention with nutritional supplements may have long-lasting positive effects on diet-related glucose metabolism and potentially mediate the progression of neurodegeneration in middle-aged and elderly people. We previously reported that cyanidin 3-*O*-*β*-galactoside (Cy3Gal), an anthocyanin from black chokeberry (*Aronia melanocarpa* (Michx.) Elliott), alleviated cognitive impairment in aging mice through regulating brain energy metabolism. However, it remains unclear whether Cy3Gal can also exert beneficial effects in mice fed with a high-fat/high-sugar diet. Here we revealed that Cy3Gal treatment conserved the health of neurons and synapses, as well as cognitive function of mice. Furthermore, we observed that Cy3Gal effectively improved glucose uptake and metabolism of skeletal muscle by enhancing glycolysis both *in vivo* and *in vitro* models, which is essential for maintaining a stable glucose supply to the brain. Additionally, Cy3Gal significantly increased the levels of glucose-derived tricarboxylic acid cycle intermediates in the mice brain ($P < 0.05$), and regulated the activities of mitochondrial respiratory chain complexes ($P < 0.01$). The positive influence on peripheral and brain bioenergetics explained how the Cy3Gal exerted neuroprotective effect. In conclusion, our study illustrated that early dietary intervention of Cy3Gal had significant advantages in terms of neuroprotection and cognition under the challenge of HFHS diet-induced glucose metabolism disorder.



## 1. Introduction

Age-related neurodegenerative diseases (NDs), such as Alzheimer's disease (AD) and Parkinson's disease (PD), are the common causes of chronic diseases, cognitive impairment, and death in the elderly[1]. With the accelerating process of population aging, NDs are expected to surpass cancer and become the second leading cause of disease-related death worldwide, and cognitive decline is one of the major risk factors for prevalent NDs[2]. NDs bring a heavy burden to the family and society. Unfortunately, there is no proven effective treatment available to prevent or slow down progression of these disorders. Complicating matters further, owing to the occult nature of NDs[3], most patients are diagnosed at a moderate to severe stage, leaving little room for a viable solution. Therefore, early identification and timely intervention of individuals at risk for these common forms of NDs are crucial factors in maximizing cognitive and brain health benefits while reducing mortality rates[4].

[1] These two authors should be considered joint first authors of the paper.
[*] Corresponding authors.
*E-mail addresses*: lijingming@cau.edu.cn (J.M. Li); yangxq@gzhu.edu.cn (X.Q. Yang)
Peer review under responsibility of Beijing Academy of Food Sciences.

Publishing services by Tsinghua University Press

http://doi.org/10.26599/FSHW.2024.9250275

The development of chronic NDs is influenced by various factors. Some studies have focused on typical pathological markers of NDs, such as neuronal degeneration and death, abnormal protein aggregation, neuroinflammation, and impaired axonal transport[5]. More specifically, some studies have focused on the brain $\beta$-amyloid plaque deposition and microtubule-associated protein tau tangle of AD[5]. Nutritional interventions have been explored as strategies to counteract these pathological processes, and most drug candidates have been designed to target these markers in order to intervene and treat NDs[6-7]. Unfortunately, the effects of these interventions have often been unsatisfactory or have failed to pass clinical trials[8]. Meanwhile, there has been increasing evidence to suggest that impaired brain energy metabolism plays a crucial role in the early stages of NDs, particularly in AD and PD, which drives the downstream neurodegeneration and cognitive impairment[9]. However, the brain, despite accounting for only about 2% of body weight, requires a disproportionately high amount of energy supply (approximately 20% of glucose-derived energy) to maintain normal physiological function[10], most of which is produced by neurons through glycolysis and mitochondrial oxidative phosphorylation (OXPHOS)[11]. It is most likely to affect brain once the body's energy metabolism is abnormal in mammal. When the metabolism of body is disturbed by genetic susceptibility, epigenetics and lifestyle, it can lead to changes in brain glucose utilization and mitochondrial energy conversion capacity, while these characteristics are often observed in the brain tissue of post-mortem NDs patients[12]. It is of great importance to understand the role of energy metabolism and mitochondrial function regulation in the pathological mechanism of NDs. Modern unhealthy diets and lifestyles have significantly increased the risk of people suffering from metabolic disorders such as type 2 diabetes mellitus (T2DM) and obesity, especially abnormal glucose and lipid metabolism that accelerates the process of NDs[13-14]. Early intervention in early to middle adulthood to maintain healthy levels of high-density lipoprotein (HDL), triglyceride (TG) and glucose levels, especially blood glucose levels, can improve cognitive ability and reduce the risk of suffering from NDs[15]. Implementing preventive measures targeting glucose metabolism disorders in the early stages may have a significant impact on reducing the incidence of NDs decades later[16]. Natural compounds, such as lycopene, polyphenols and saponins, displayed the potential effects of improving the cognitive impairment of mice induced by high-calorie diet[16-17]. These findings suggest that preserving and/or restoring brain energy status against long-term high-calorie diet is supposed to be an effective way to alleviate nervous system dysfunction and reduce the risk of cognitive impairment.

Our previous study has proved that the early intervention of cyanidin 3-*O*-$\beta$-galactoside (Cy3Gal) displayed beneficial effects on brain energy metabolism in aging mice through enhancing the glucose uptake and improving the mitochondrial membrane permeability of the brain[18]. The healthy benefits were closely associated with neuroprotective function and cognitive improvement of aging mice[18]. However, it is not well understood whether Cy3Gal can improve peripheral blood glucose metabolism and subsequently promote energy metabolism in the brain. Furthermore, we focused on the neuroprotective effects of early dietary intervention of Cy3Gal and the impact on cognitive dysfunction in diet-induced glucose metabolism disorder mice. In this study, a high-fat/high-sugar (HFHS) diet combined with intraperitoneal injection of streptozotocin was used to build a mouse model of glucose-metabolism disorder. Following six weeks of oral administration (Cy3Gal), neuroprotective effects were assessed by behavioral test, histopathological analysis, and targeted metabolomics of glucose metabolism.

## 2. Materials and methods

### 2.1 Chemicals

Cy3Gal (≥ 95% purity) was purified from black chokeberry (*Aronia melanocarpa* (Michx.) Elliott) in our previous study[19]. High-density lipoprotein cholesterol (HDL-C), low-density lipoprotein cholesterol (LDL-C), TG, glucose, lactate, and glycogen assay kits were purchased from Nanjing Jiancheng Bioengineering Research Institute (Nanjing, China). Synaptophysin (Syn) rabbit polyclonal antibody was purchased from Wuhan Sanying Proteintech Group, Inc. (Wuhan, China). Postsynaptic density protein (PSD-95) rabbit monoclonal antibody, bicinchoninic acid (BCA) assay kit, Nissl staining kit, tissue mitochondria isolation kit, membrane protein extraction kit, cell counting kit-8 (CCK-8), and glucose transporter 4 (GLUT4) rabbit polyclonal antibody were purchased from Beyotime Biotechnology Co., Ltd. (Shanghai, China). A$\beta_{1\text{-}42}$ antibody was purchased from Abcam company (Cambridge, UK). Mitochondria respiratory chain complex I, III, IV, V ELISA kits were purchased from Shanghai Enzyme-linked Biotechnology Co., Ltd. (Shanghai, China). Diaminobenzidine (DAB) kit was purchased from Dako Denmark A/S (Glostrup, Denmark). Dulbecco's modified Eagle's medium (DMEM)-low glucose, DMEM-high glucose, fetal bovine serum (FBS), and horse serum were purchased from HyClone Co. (South Logan, UT, USA). Phosphate buffered saline (PBS) and bovine serum albumin (BSA, free fatty acids-free) were purchased from Beijing Solarbio Science & Technology Co., Ltd. (Beijing, China). All standards (≥ 95% purity) of glucose-derived metabolic intermediates were purchased from Sigma Aldrich Co. (St. Louis, MO, USA). All HPLC grade reagents were purchased from ANPEL Laboratory Technologies (Shanghai) Inc. (Shanghai, China). All other reagents were of the highest grade commercially available.

### 2.2 Experimental animal and intervention protocol

4-Week-old male C57BL/6N mice ((20 ± 2) g) were purchased by Beijing Vital River Laboratory Animal Technology Co., Ltd. (SCXK (Jing) 2021-0006, Beijing, China). All mice were kept in a temperature-controlled ((22 ± 2) ℃) animal facility under a 12 h dark-light cycle. Water and food were available *ad libitum*. After adaption, 48 mice were randomly divided into 2 groups as following, Control: 12 mice were fed with a normal diet; Model: 36 mice were fed with HFHS (60 kcal % fat, 20 kcal % sucrose) diet. Four weeks later, after fasting for 12 h, the mice in Model group were intraperitoneally injected with streptozotocin (STZ, 50 mg/kg b.w.) for 3 days[20] to damage the function of $\beta$-cells and reduce insulin synthesis and secretion, thereby accelerating glucose metabolism disorders[21]. The Control group mice were intraperitoneally injected with normal saline. One week later, the fasting blood glucose (FBG) of all the mice was measured. Mice with FBG levels ≤ 8.8 mmol/L in the Control group were chosen as CK group, which were orally administrated with 0.2 mL sterile water and fed with normal diet. Mice with FBG levels ≥ 11.1 mmol/L were randomly divided into

model, Cy3Gal-Low and Cy3Gal-High groups. The model group mice were orally administrated with 0.2 mL sterile water and fed with HFHS diet. The Cy3Gal-Low and Cy3Gal-High groups mice were orally administrated with low or high dose of Cy3Gal (25 or 50 mg/(kg·day)) dissolved in 0.2 mL sterile water and fed with HFHS diet. Body weight measurements were performed once a week. All mice were subjected to behavioral tests after 6 weeks of administration and scacrificed after the last behavioral test. All experiments were approved by the Animal Ethical and Welfare Committee (No. NKYY-DWLL-2021-090).

### 2.3 Oral glucose tolerance test (OGTT)

After 6 weeks of diet intervention, the OGTT was carried out as previously described[22]. Mice were fasted overnight and then glucose (1.0 g/kg b.w.) was orally administered. Blood glucose from the tail vein was measured with glucose oxidase method at 0, 30, 60, 90, and 120 min after glucose challenge.

### 2.4 Y maze test

After 6 weeks of diet intervention, the Y maze test was performed as previously described with minor modifications[23]. The Y-shaped maze consists of three arms (8 cm × 30 cm × 15 cm, width × length × height) with a 120° angle from each other. Three arms were randomly designated as start arm, food arm and wrong arm. The test includes adaptation, training and testing trials. Adaptation trial: all the mice were fasted for 24 h before the experiment. The food was put into the three arms and a mouse was placed at the start arm to find food for 6 min. The 2 adaptation trials were conducted in one day, with a minimum 2-h interval separating them. Training trial: after two adaptation trials, the training trials were conducted twice daily for 2 days. Food was put into only one arm and a mouse was placed at the starting arm to explore arbitrarily to find the food for 6 min. Testing trial: after training trials, the food was withdrawn from the Y maze. The mice were put into the starting arm and allowed to explore arbitrarily for 6 min. The camera system recorded the behavior of the animals. The times and total distance of mice entering the food arm within 6 min were recorded as the indexes. Recognition of the food arm from three arms is considered to have the good spatial recognition and memory abilities. All the maze arms were cleaned with 75% ethanol between trials.

### 2.5 Serum content assays

After Y maze test, blood was collected from the inner canthus vein of mice. After standing at 4 ℃ for 4 h, the blood was centrifuged at 3 500 r/min for 15 min, and the supernatant was collected and stored at −20 ℃. The levels of HDL-C, LDL-C, and TG were determined according to the instructions of the assay kits.

### 2.6 Mitochondria isolation and biochemical analysis

Mitochondria were purified from the fresh mice brain tissues according to the instructions of the assay kits, and mitochondria respiratory chain complexes (I, III, IV, V) were determined by ELISA kits.

### 2.7 Nissl staining

Mice were euthanized and perfused with normal saline. Then the brains were taken out and preserved in 4% paraformaldehyde. Serial coronal sections with a thickness of 25 μm were cut using a cryostat (Leica Microsystems, Wetzlar, Germany). The sections were washed twice for 5 min in 0.01 mol/L PBS and incubated in 1% toluidine blue staining solution for 5−10 min at 20−25 ℃. Afterwards, the sections were rinsed in distilled water, soaked in 95% ethanol for 30 min, and dehydrated in 100% ethanol. After dehydration, the sections were placed in xylene and cover-slipped using resin medium. The number of neurons in hippocampus and cerebral cortex were quantified using ImageJ-Pro Plus software (developed by Wayne Rasband from NIH, USA).

### 2.8 Immunohistochemical staining

Fixed brain sections were immersed in xylene and gradient ethanol for deparaffinization and rehydration. Afterward, the brain pieces were placed in citric acid (pH 6.0) antigen retrieval buffer for antigen retrieval, and shaken 3 times for 5 min each on the decolorization shaker. Then, the slices were put into 3% hydrogen peroxide and incubated at 25 ℃ in darkness for 25 min to block endogenous peroxidase activity. Then, the same operation was performed in PBS. 3% BSA was added to evenly cover the tissue, and the tissues were sealed for 30 min at 25 ℃ (primary antibody was sealed with normal rabbit serum from goat source, and other sources were sealed with BSA). $A\beta_{1\text{-}42}$ antibody diluent (1∶100) incubated sections at 4 ℃ overnight. The sections were washed by PBS before being incubated with the corresponding secondary antibody at 25 ℃ for 50 min. The washing step was repeated using PBS, and DAB was utilized for dyeing prepared samples. Subsequently, hematoxylin was used to re-dye, and neutral resin was used to block the brain slices. Eventually, images from stained sections were employed by the optical microscope (Olympus, Tokyo, Japan). Images were analyzed with ImageJ software.

### 2.9 Immunofluorescence staining

The procedure is similar to immunohistochemistry. Briefly, fixed brain sections were rehydrated, and exposed to antigen retrieval in citric acid antigen repair buffer (pH 6.0) for 10 min at 95−100 ℃. Tissues were then blocked with BSA for 30 min, and incubated in primary antibody (anti-Syn, 1∶500; anti-PSD95, 1∶200 at 4 ℃) and florescent secondary antibody (goat anti-rabbit, 1∶400, 2 h at 25 ℃). After incubation, nuclear staining was performed with 4',6-diamidino-2-phenylindole (DAPI). Sections were visualized using fluorescent microscope (Olympus, Tokyo, Japan). Images were analyzed with ImageJ software.

### 2.10 Metabolomic analysis

Isolated calf muscle and brain tissues were flash frozen in liquid nitrogen and stored at −80 ℃ until analysis. A total of 60 mg muscle tissue or 90 mg brain tissue were added with precooled methanol/acetonitrile/water (1:1:1, *V*/*V*). After grinding, 600 μL precooling methanol/acetonitrile/water (1:1:1, *V*/*V*) was added to extract by

ultrasonic in ice bath for 1 h. The samples were obtained by centrifugation and vacuum freeze-drying, which were then added with acetonitrile aqueous solution (1:1, *V*/*V*) to dissolve and supplemented with the internal standard (*L*-glutamate-$d_5$). After centrifugation, the supernatant was taken for detection. Shimadzu Nexera X2 LC-30AD equipped with Waters UPLC BEH Amide column (2.1 mm × 100 mm, 1.7 μm) was used for separation. Mobile phase: A was 5% acetonitrile aqueous solution (pH 9), containing 10 mmol/L ammonium acetate; B was 95% acetonitrile aqueous solution (pH 9), containing 10 mmol/L ammonium acetate. The automatic sampler temperature was 4 ℃, the column temperature was 40 ℃, the flow rate was 300 μL/min, and the injection volume was 5 μL. The gradient was as follows: 95% B (0−2 min); 95%−70% B (2−9 min); 70%−30% B (9−10 min); 30% B (10−11 min); 30%−95% B (11−11.5 min); 95% B (11.5−15 min). Mass spectrometry was performed in positive/negative ion mode using Qtrap 5 500 mass spectrometer (AB SCIEX). The electrospray ionization source operation parameters were as follows: source temperature 550 ℃, ion spray voltage 5 500 V (positive), −4 500 V (negative). Multiple reaction monitoring (MRM) mode was used to detect the ion pair to be tested. The chromatographic peak area and retention time were extracted by MultiQuant software. All the intermediates were identified and quantified according to the standards (Tables S1 and S2).

### 2.11 C2C12 cell culture, differentiation, and treatment

C2C12 cells (BeNa Culture Collection, Beijing, China) were maintained in DMEM-low glucose (containing 5.5 mmol/L glucose) with 10% FBS and 1% penicillin/streptomycin until about 80% confluence. For differentiation, cells were detached by trypsin and then plated in 6 cm culture dishes or 96-well plates and incubated in differentiation media (DMEM-low glucose containing 2% horse serum and 1% penicillin/streptomycin). The differentiation media was changed daily until cells were fully differentiated (around day 5).

The cell viability was detected by CCK-8 method. Cells were seeded into 96-well plates (100 μL/well) and starved with DMEM-low glucose containing 1% BSA for 10−12 h, then treated with different concentrations of Cy3Gal (5, 10, 20, 50, 100 μmol/L) dissolved in DMEM-high glucose (containing 25 mmol/L glucose) with 1% BSA. After incubation for 24 and 48 h, the cells were washed twice with PBS and 100 μL DMEM-low glucose and 10 μL CCK-8 was added for an additional 1−2 h. Finally, the cell viability was determined according to the instructions.

The glucose consumption, lactate production, and glycogen level of C2C12 cells were determined by assay kits, respectively. Briefly, cells were seeded into 6 cm culture dishes, and were cultured in Cy3Gal with 1% BSA for 36 h after differentiation. Afterward, the culture medium was collected to detect the concentrations of glucose and lactate and the cells were collected to detect the glycogen level. To examine the effects of Cy3Gal on GLUT4 membrane translocation in C2C12 cells, cells were cultured in Cy3Gal with 1% BSA for 36 h after differentiation. Subsequently, the cells were collected after being stimulated with 100 nmol/L insulin for 30 min. The membrane protein of the cells was extracted according to instructions. The expression of GLUT4 was examined by Western blotting. The protein samples were separated by sodium dodecyl sulfate-polyacrylamide gel electrophoresis (SDS-PAGE), transferred to the polyvinylidene fluoride (PVDF) membrane, and sealed with 5% skim milk for 2 h. The PVDF membrane was then incubated with specific primary antibody (anti-GLUT4, 1:1 000) at 4 ℃. Horseradish peroxidase binding secondary antibodies were incubated with the PVDF membrane. The proteins were visualized by chemiluminescence reagents and analyzed by the gel recording system (GelDoc It 310 imaging system).

### 2.12 Statistical analysis

Data are presented as mean ± standard deviations. The test data were processed by One-way ANOVA using the SPSS version 20.0 software package. Multiple comparisons of the data were performed via Tukey's test, which was used to compute significant differences at $P < 0.05$, $P < 0.01$ and $P < 0.001$.

## 3. Results

### 3.1 Cy3Gal had significant beneficial effects on blood glucose and lipid control

We first examined whether Cy3Gal could improve peripheral energy homeostasis in overnutrition mice. A vehicle solution and Cy3Gal were administered orally to 12-week-old mice for 6 weeks, following by a behavioral test and biochemical analysis (Fig. 1A). Mice in Model group had a significantly higher weight growth rate and body weight than mice fed with normal diet, while Cy3Gal-Low and Cy3Gal-High treatments partially significantly reduced the body weight and body weight growth rate in HFHS-fed mice (Figs. 1B, C). Furthermore, Cy3Gal-High treated mice showed improved glucose tolerance and decreased FBG concentration relative to Model group, suggesting improved glucose control, whereas Cy3Gal-Low only strongly reversed the increase in FBG concentration of HFHS diet induction (Figs. 1D, E). To evaluate the effects of Cy3Gal on lipid homeostasis, serum LDL-C, TG, and HDL-C of mice were measured. Compared with CK mice, HFHS diet resulted in significant increases in LDL and TG levels, while Cy3Gal-Low and Cy3Gal-High treatments reversed the changes (Figs. 1F, G). Notably, Cy3Gal significantly increased serum HDL-C levels, although they were not significantly changed by HFHS diet (Fig. 1H). These results indicated that Cy3Gal had significant beneficial effects on improving glucose and lipid homeostasis of HFHS-fed mice.

### 3.2 Cy3Gal alleviated memory deficit and cognitive impairment

Afterwards, we were interested in investigating the learning and memory behaviors of mice by conducting the Y maze test (Figs. 2A and D). The total moving distance in the correct arm ($P < 0.01$, Fig. 2B) and the number of entering the correct arm in model mice were significantly reduced when compared with CK mice ($P < 0.001$, Fig. 2C), whereas Cy3Gal-High treatment significantly reversed HFHS induction ($P < 0.001$, $P < 0.01$, respectively). The results suggested Cy3Gal showed a valid dietary effect on alleviating the memory deficit and cognitive impairment in HFHS-fed mice.

### 3.3 Cy3Gal exerted neuronal protection

Memory and cognitive dysfunctions are closely related to neuronal damage in hippocampus and cerebral cortex[24]. Nissl

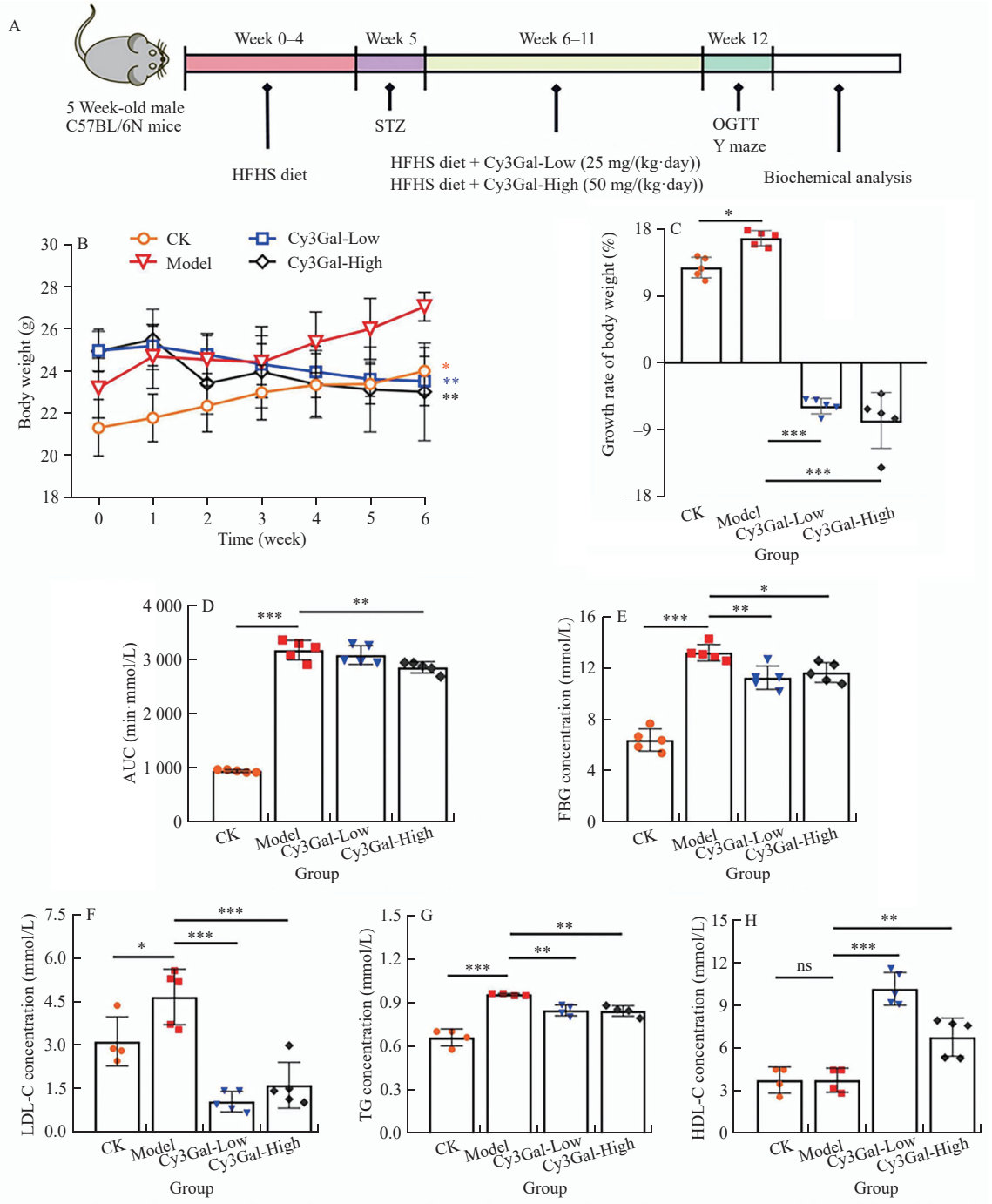


**Fig. 1** Cy3Gal improved obesity, blood glucose and lipid homeostasis in HFHS-fed mice. (A) Experimental workflow of animal treatments; (B) Body weight changes during 6 weeks of treatment ($n$ = 6 for each group); (C) Growth rate of body weight before and after 6-week Cy3Gal treatment ($n$ = 5 for each group); (D) The area under glucose curve (AUC) at the end of treatment ($n$ = 5 for each group); (E) FBG at the end of treatment ($n$ = 5 for each group); (F) Serum LDL-C levels ($n$ = 4, 5, 5, 5 for CK, Model, Cy3Gal-Low, and Cy3Gal-High groups, respectively); (G) Serum TG levels ($n$ = 4 for each group); (H) Serum HDL-C levels ($n$ = 4, 4, 5, 5 for CK, Model, Cy3Gal-Low and Cy3Gal-High groups, respectively). *$P$ < 0.05, **$P$ < 0.01, ***$P$ < 0.001, ns not significant.

staining, a staining technique using basic dye for targeting Nissl body of neuron[25], showed that the hippocampus neurons of CK mice were arranged tightly and orderly with clear nuclei, and there were clear Nissl bodies in the cytoplasm, as indicated by red arrows in Fig. 3. In contrast, numerous neurons with damaged nuclei were observed in model mice, accompanied with Nissl body loss especially in CA1 and dentate gyrus (DG) regions ($P$ < 0.001, Fig. 3B; $P$ < 0.001, Fig. 3F). However, Cy3Gal intervention significantly reduced neuronal loss in the hippocampus of mice. Cy3gal-Low intervention protected neurons from damage and apoptosis in the CA1 region of hippocampus ($P$ < 0.05, Fig. 3B). Likewise, in Cy3Gal-High group mice, the neurons exhibited normal morphology with distinct round or oval nuclei and nucleoli in the CA1, CA2, and DG regions of hippocampus, and the number of Nissl bodies increased significantly ($P$ < 0.01, Fig. 3B; $P$ < 0.05, Fig. 3C; $P$ < 0.001; Fig. 3F), although no significant effect was observed on the cells in the CA3 region

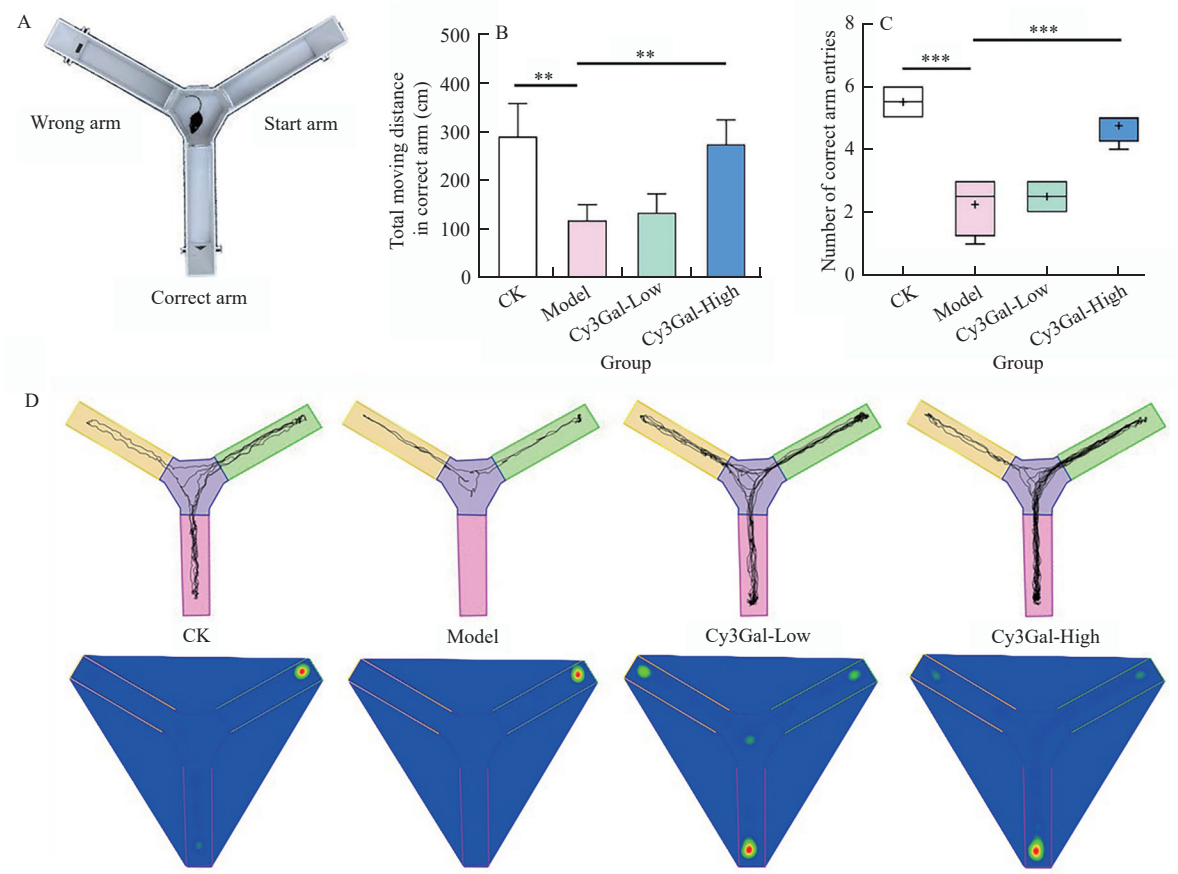


**Fig. 2** Cy3Gal improved cognitive impairments in overnourished mice ($n$ = 6). (A) Schematic diagram of Y maze. (B) The total moving distance of mice in the correct arm of Y maze. (C) The number of entering the correct arm of mice in Y maze. (D) Representative action tracks (upper panel) and heat maps of action track (lower panel) of mice among different groups in the Y maze test. $^{**}P < 0.01$, $^{***}P < 0.001$.

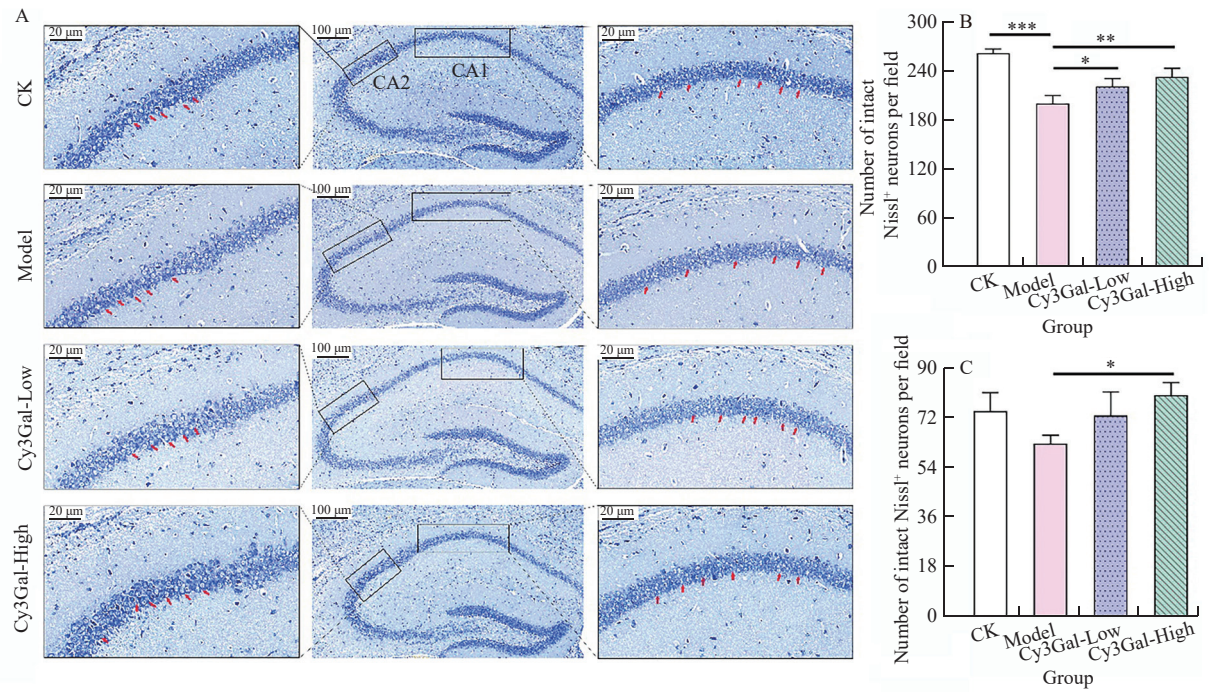


**Fig. 3** Histological examinations of the neuron in mice hippocampus ($n$ = 4). (A) Representative Nissl staining images of CA1 (left panel) and CA2 (right panel) regions from different groups. (B, C) Analysis of Nissl positive neurons in CA1 and CA2 regions. (D) Representative Nissl staining images of CA3 (left panel) and DG (right panel) regions from different groups. (E, F) Analysis of Nissl positive neurons in CA3 and DG regions. The red arrows indicated neurons. $^{*}P < 0.05$, $^{**}P < 0.01$, $^{***}P < 0.001$.

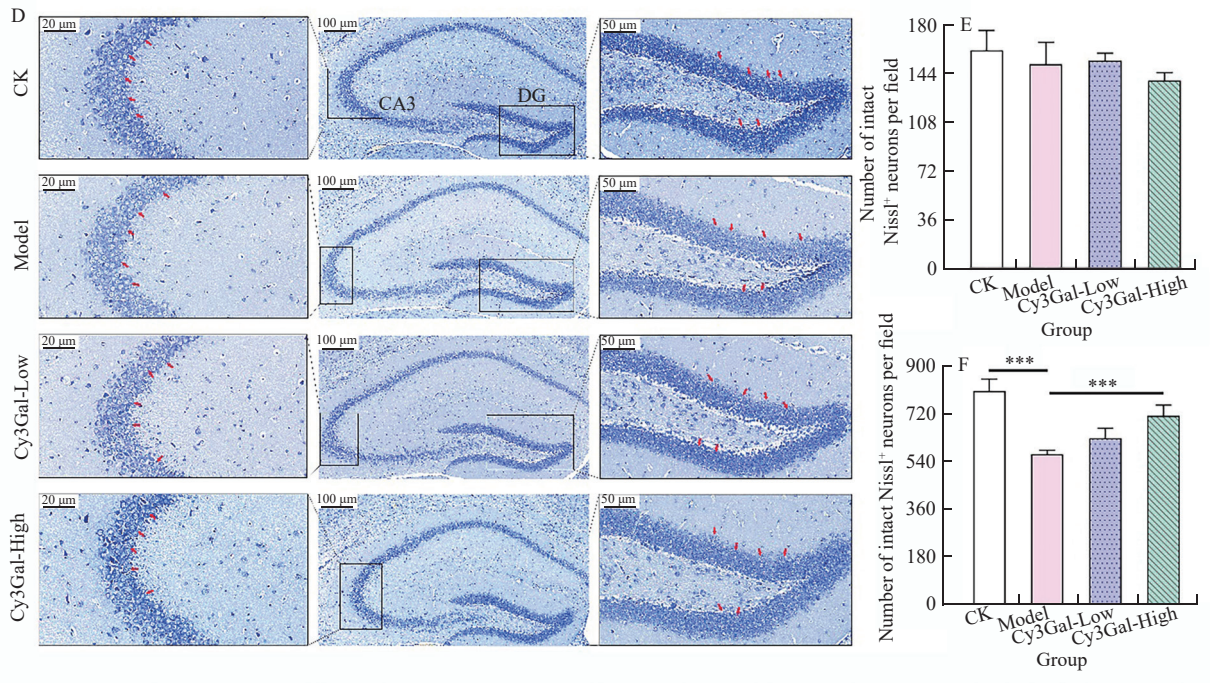


**Fig. 3** (*continued*)

($P$ > 0.05, Fig. 3E). In addition, the results showed a prospective Cy3Gal-mediated improvement on the neuron degeneration and loss in cerebral cortex of HFHS-fed mice (Fig. S1). Collectively, those results suggested that Cy3Gal reduced the neuronal damage and apoptosis, and promoted cognitive functions in HFHS-fed mice.

### 3.4 Cy3Gal enhanced synaptic plasticity

Synapse is the basis of neural circuit, and plays a vital role in cognition and behavior, in which neurons communicate. While abnormal synaptic plasticity and neuronal apoptosis usually occur in the early stage of cognitive impairment[24,26]. In addition, synaptic activities require high bioenergy demands[27]. HFHS diet led to marked decreases in the expressions of Syn and PSD 95 in the hippocampus ($P$ < 0.05, $P$ < 0.001, respectively), and the synaptic density was decreased compared with CK mice (Fig. 4). While Cy3Gal intervention strongly reversed the changes. The synapses were densely distributed in the hippocampus, and the fluorescence intensity of Syn and PSD 95 were significantly increased in Cy3Gal-Low group mice ($P$ < 0.001, Fig. 4A; $P$ < 0.05, Fig. 4B, respectively). Cy3Gal-High intervention increased Syn expression in the hippocampus ($P$ < 0.01, Fig. 4B). These results indicated a great effect of Cy3Gal on ameliorating HFHS diet-induced synaptic plasticity deficiency and synaptic dysfunction.

Studies have provided evidence that the clearance rate of $\beta$-amyloid is significantly reduced in the brain of diabetic animals spontaneously or induced by STZ[28]. Therefore, we made an insight into the associations between levels of $\beta$-amyloid and synapse impairment in the hippocampus and cerebral cortex. HFHS-fed mice showed mildly increases in the $\beta$-amyloid levels of hippocampus CA1, CA2, and CA3 regions compared with CK mice ($P$ > 0.05). Likewise, effects of Cy3Gal treatment on $\beta$-amyloid levels in hippocampus CA1, CA2, and CA3 regions were insignificant ($P$ > 0.05). In accordance, accumulation of $\beta$-amyloid did not show significant changes in cerebral cortex of mice with both HFHS diet and Cy3Gal treatment ($P$ > 0.05, Fig. S2).

### 3.5 Cy3Gal improved blood glucose absorption and metabolism by enhancing glycolysis in skeletal muscle

Given that skeletal muscle is the major site of glucose and lipid uptake, we performed a targeted analysis of glucose intermediates in skeletal muscle to investigate the effects of Cy3Gal on the peripheral glucose metabolic homeostasis in HFHS-fed mice. Compared with model mice, the level of lactate in skeletal muscle was increased significantly by Cy3Gal-Low treatment (fold change of Cy3Gal-Low and model ($FC_{Low}$) = 1.06, $P$ < 0.05), although there was no significant difference between Model and CK groups. The lactate level also did not show major changes in Cy3Gal-High group compared to Model group ($P$ > 0.05, Fig. 5A). Additionally, Cy3Gal-Low and Cy3Gal-High treatment significantly enhanced the $NAD^+$/NADH ratio ($FC_{Low}$ = 1.42, $P$ < 0.05; Fold change of Cy3Gal-High and model ($FC_{High}$) = 1.44, $P$ < 0.05) compared with Model group (Fig. 5B). Interestingly, significantly increases of $NAD^+$/NADH ratio in Cy3Gal treated mice were also observed compared with CK mice ($P$ < 0.01, Fig. 5B), which suggested that Cy3Gal might affect the glycolysis in overnourished mice. Furthermore, levels of glycolysis intermediates in HFHS-fed mice decreased compared with CK mice, including glucose 6-phosphate, dihydroxyacetone phosphate, glyceraldehyde 3-phosphate, phosphoenolpyruvate and pyruvate, the levels of which were decreased by 53.89%, 74.52%, 37.37%, 29.87%, and 16.39%, respectively. However, Cy3Gal treatment significantly increased the levels of these intermediates (Figs. 5C-G). Additionally, the results also showed that the AMP/ATP ratio in model mice was 2.35 times higher than that in CK mice ($P$ < 0.001). Compared with the model mice, the AMP/ATP ratio showed a Cy3Gal dose-dependent decrease ($FC_{Low}$ = 1.83, $P$ < 0.001; $FC_{High}$ = 2.84, $P$ < 0.001; Fig. 5I). These data demonstrated

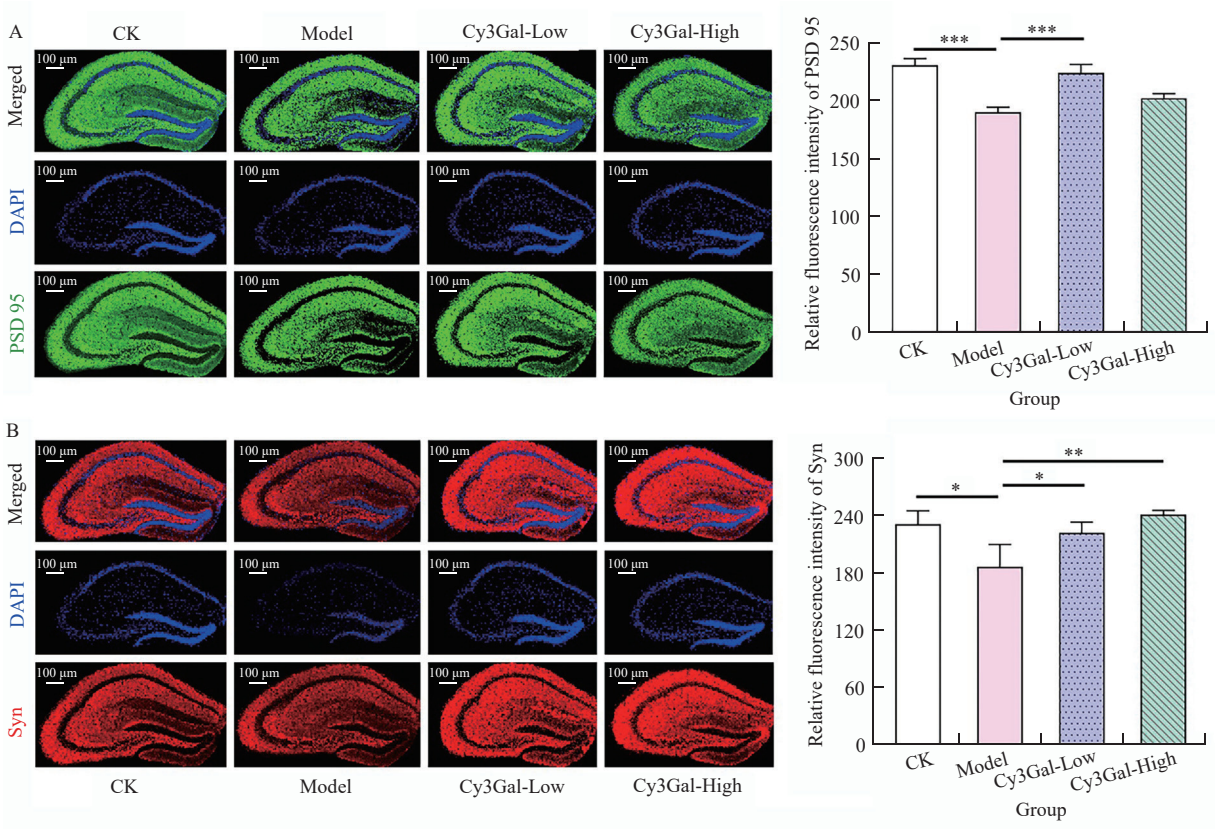


**Fig. 4** Cy3Gal protected synapses from damage in overnourished mice ($n$ = 3). (A) Representative immunofluorescence staining sections of PSD 95 (green) in the brain (left) and quantification of positive area based on immunofluorescence staining sections by ImageJ software (right). (B) Representative immunofluorescence staining sections of Syn (red) in the brain (left) and quantification of positive area based on immunofluorescence staining sections by ImageJ software (right). Cell nuclei were stained with DAPI (blue). *$P$ < 0.05, **$P$ < 0.01, ***$P$ < 0.001.

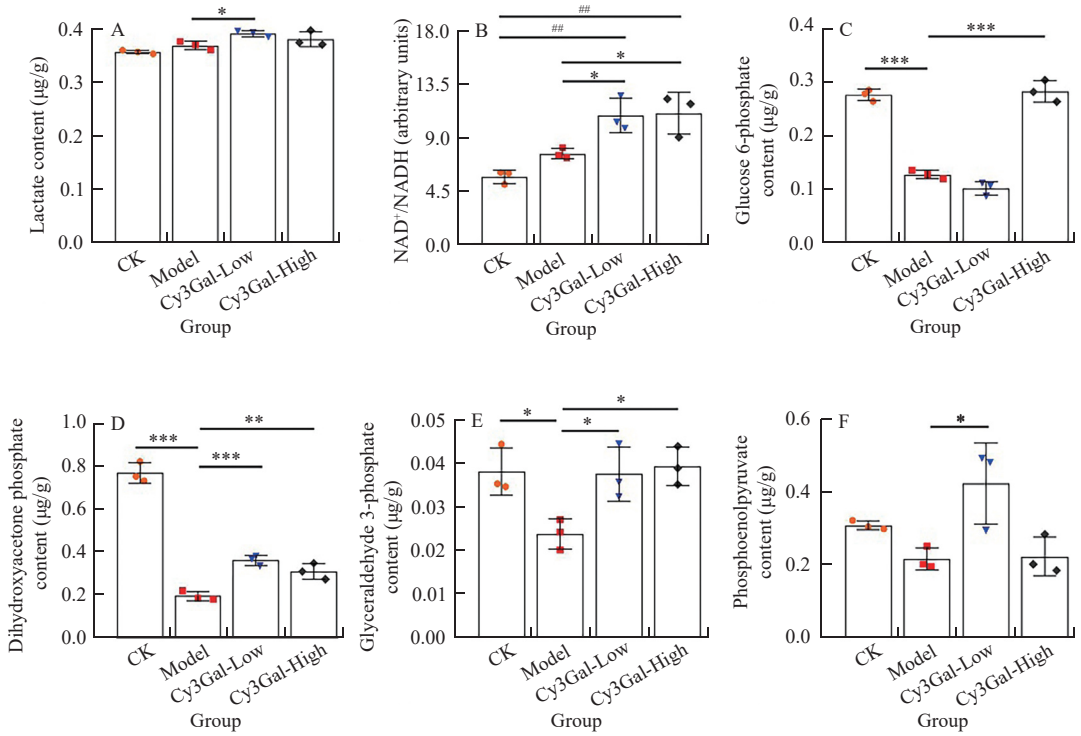


**Fig. 5** Cy3Gal enhanced glycolysis of skeletal muscle in overnourished mice ($n$ = 3). (A) Levels of lactate among different groups; (B) $NAD^+$/NADH ratio among different groups; (C-H) Levels of glycolysis related intermediates among different groups; (I) AMP/ATP ratio among different groups. (J) Effects of Cy3Gal on tricarboxylic acid (TCA) circle related intermediates in skeletal muscle among different groups. *$P$ < 0.05, **$P$ < 0.01, ***$P$ < 0.001; $^{\#\#}P$ < 0.01.

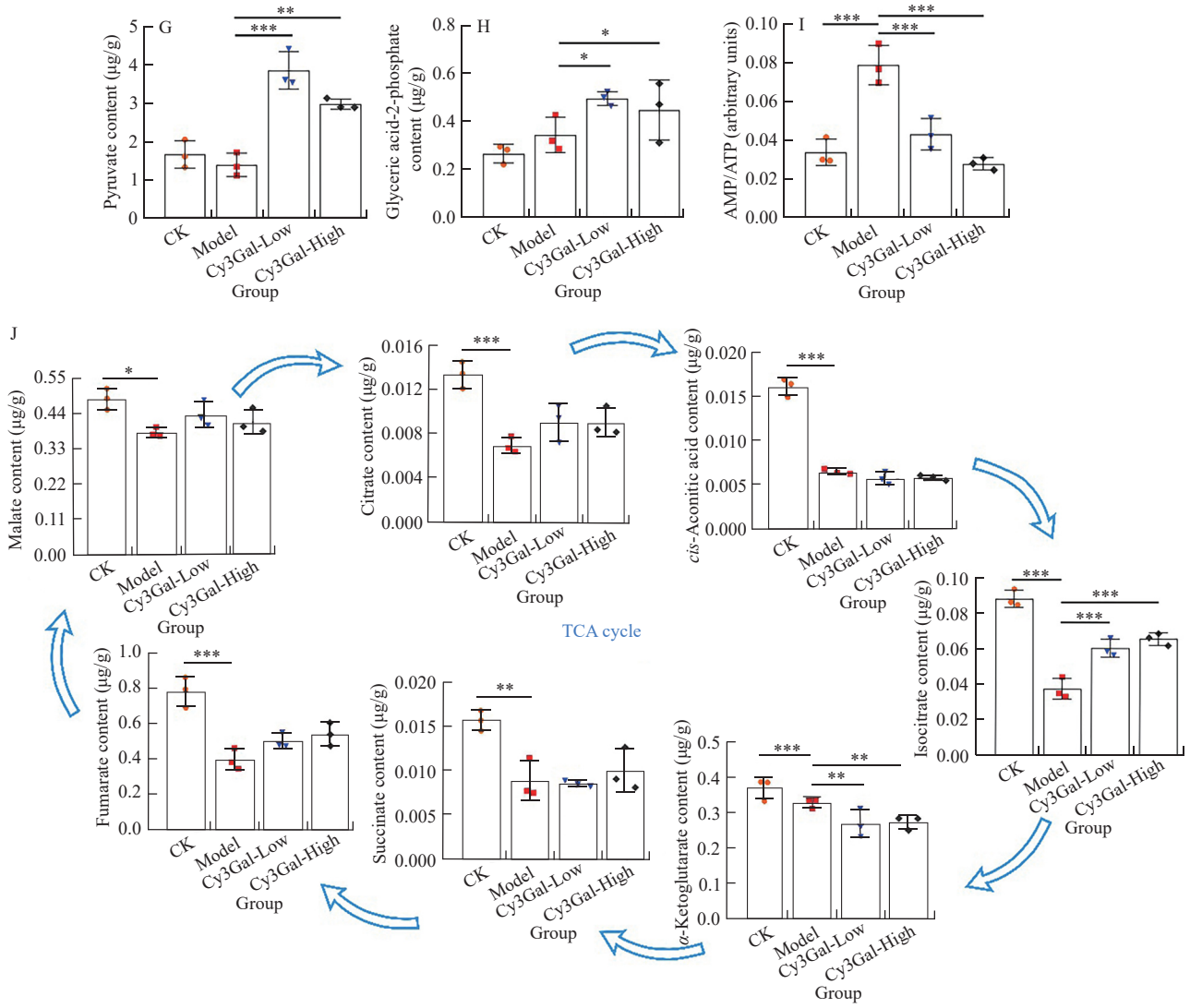


**Fig. 5** (*continued*)

that Cy3Gal modulated glucose intermediates of the glycolysis in skeletal muscle.

Levels of pyruvate, the key intermediate connecting glycolysis and TCA cycle, were markedly increased by Cy3Gal-Low and Cy3Gal-High treatments ($P < 0.001$, $P < 0.01$, respectively; Fig. 5G). We next focused on the effects of Cy3Gal on TCA cycle in skeletal muscle. Compared with CK mice, levels of citrate, *cis*-aconitic acid, isocitrate, *α*-ketoglutarate, succinate, fumarate, and malate were significantly reduced in model mice. However, significant changes only in isocitrate and *α*-ketoglutarate were observed between model and Cy3Gal-treated mice (Fig. 5J). Notably, levels of *α*-ketoglutarate were decreased significantly by Cy3Gal intervention (Fig. 5J), which might be related to the Cy3Gal-induced high $NAD^+$/NADH ratio (Fig. 5B).

Afterwards, we employed C2C12 myotubes to validate effects of Cy3Gal on glucose metabolism in skeletal muscle, and 5−100 μmol/L Cy3Gal significantly increased the cell viability ($P < 0.001$, Fig. S3). Based on the consideration of glucose absorption and metabolism perspective, 20 and 50 μmol/L concentrations of Cy3Gal were selected for further experiment. Consistently, the glucose consumption rate ($P < 0.01$, Fig. 6A), lactate production ($P < 0.05$, Fig. 6B), and glycogen level ($P < 0.05$, Fig. 6C) in differentiated C2C12 myotubes were significantly increased by 20 μmol/L-Cy3Gal treatment, and 50 μmol/L-Cy3Gal strongly enhanced glycogen synthesis relative to control C2C12 cells ($P < 0.001$, Fig. 6C).

GLUT4 is essential to the glucose uptake in skeletal muscle, and GLUT4 translocation from the cytosol to the cell membrane is considered to be the rate-limiting step in insulin-and contraction-stimulated glucose uptake[29]. Our results demonstrated that GLUT4 expression in C2C12 cell membrane was significantly increased by 20 μmol/L Cy3Gal ($P < 0.05$, Fig. 6D), suggesting Cy3Gal promoted GLUT4 membrane translocation. The enriched GLUT4 in cell membrane was consistent with the observed enhanced glucose metabolism of C2C12 cells (Fig. 6A). Overall, these data demonstrated a promising efficacy of Cy3Gal to improve glucose homeostasis by enhancing glycolysis.

### 3.6 *Cy3Gal enhanced TCA cycle metabolism in brain*

Impaired glucose metabolism in the brain can cause dysregulated synaptic signal transduction and dysfunctional energy supply to neurons

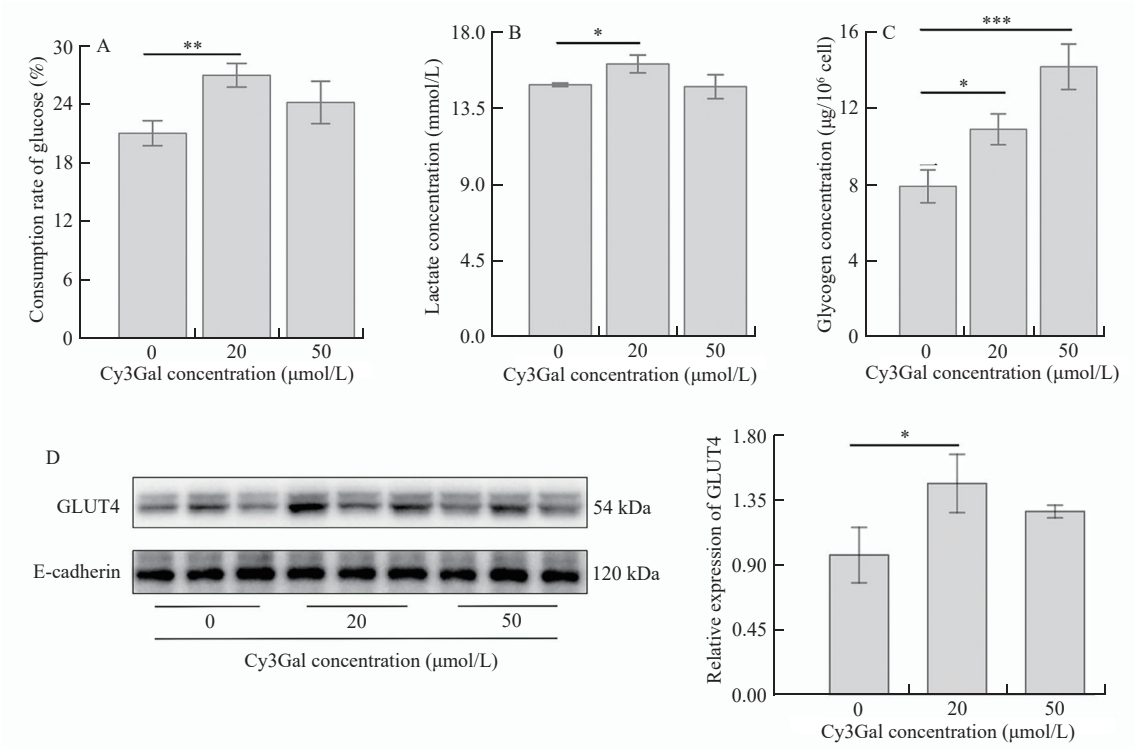


**Fig. 6** Cy3Gal promoted glucose uptake and utilization in C2C12 myotubes exposed to high glucose ($n = 3$). (A) Effects of Cy3Gal on the glucose consumption of C2C12 myotubes. (B) Effects of Cy3Gal on the lactate production of C2C12 myotubes. (C) Effects of Cy3Gal on the glycogen synthesis capacity of C2C12 myotubes. (D) Effects of Cy3Gal on the GLUT4 levels in membrane of C2C12 myotubes under high glucose and insulin stimulation. Representative Western blots of GLUT4 protein (left panel); Relative optical density of GLUT4 protein (right panel). *$P < 0.05$, **$P < 0.01$, ***$P < 0.001$.

by mitochondrial dysfunction, finally resulting in cognitive impairment and even NDs[10]. ATP required by neurons is mainly produced in mitochondrial OXPHOS through glucose derived-TCA cycle[30]. Therefore, we examined glucose metabolism in mice brain. Firstly, apart from succinate and succinate-CoA and malate, significant changes in the levels of eight TCA cycle intermediates were observed in Model group relative to CK group (Figs. 7A-L). Different from skeletal muscle, Cy3Gal intervention had a close correlation with increased TCA cycle intermediate levels in mice brain, including pyruvate ($FC_{Low} = 5.97$, $P < 0.01$; $FC_{High} = 4.19$, $P < 0.001$), oxaloacetate ($FC_{Low} = 1.56$, $P < 0.01$; $FC_{High} = 1.79$, $P < 0.001$), isocitrate ($FC_{Low} = 4.02$, $P < 0.001$; $FC_{High} = 5.09$, $P < 0.001$), succinate-CoA ($FC_{Low} = 6.47$, $P < 0.001$; $FC_{High} = 4.34$, $P < 0.001$), acetyl-CoA, citrate, *cis*-aconitate, $\alpha$-ketoglutarate, succinate, fumarate and malate (Figs. 7A-K). Meanwhile, the AMP/ATP ratio in the Model group was significantly elevated in comparison to the CK mice ($P < 0.01$). In contrast, after Cy3Gal-Low and Cy3Gal-High intervention, the AMP/ATP ratios was significantly reduced by 83.73% and 79.55%, respectively (Fig. 7L). The data suggested that Cy3Gal promoted ATP production in the brain of HFHS-fed mice.

However, there was no dynamic change in lactate production in mice brain among each group (Fig. 7K). Therefore, we further analyzed the $NAD^+$ and NADH. The $NAD^+$ level and $NAD^+$/NADH ratio decreased slightly in model mice compared with CK mice ($P > 0.05$; Figs. 7M, N). Remarkably, Cy3Gal markedly increased the $NAD^+$ levels ($P < 0.001$, Fig. 7M) and $NAD^+$/NADH ratios ($P < 0.001$, Fig. 7N) in HFHS-fed mice, which was consistent with the observed increases of $NAD^+$/NADH ratio in skeletal muscle. In addition, the levels of glycolysis intermediates in brain were increased in Cy3Gal-treated mice compared with HFHS-fed mice, including glucose 6-phosphate, fructose 1,6-diphosphate, glyceric acid 3-phosphate, glyceric acid 2-phosphate and phosphoenolpyruvate (Fig. 7K). While there was no consistent dietary effect induced by HFHS-diet feeding relative to CK mice. These results indicated that Cy3Gal intervention promoted the glucose metabolism towards TCA cycle and provided enough energy for neuron in HFHS-fed mice.

### *3.7 Cy3Gal activated mitochondrial respiratory chain complexes in brain OXPHOS system*

Mitochondrial respiratory chain complexes play important roles in energy conversion. The most abundant and important respiratory chain complexes in mammals are complex I, III and IV, which combine with complex V form OXPHOS system to synthesize ATP[31]. Hence, we conducted ELISA to measure the activities of these complex in mitochondria from brain. For complex I, IV, and V, we observed HFHS feeding significantly reduced their activities relative to CK group ($P < 0.001$, $P < 0.001$, $P < 0.01$, respectively; Fig. 8). Complex I, IV and V had obvious dysfunction where the overall electron transfer and energy production was blocked. However, Cy3Gal intervention strongly enhanced the activities of the three complexes. Interestingly, the complex III activity in model group mice was significantly increased compared with CK mice, suggesting abnormal electron transfer in the brain mitochondria of overnourished mice (Fig. 8). Meanwhile, both Cy3Gal-Low and Cy3Gal-High treatments clearly reduced the activities of complex III relative to HFHS Model group

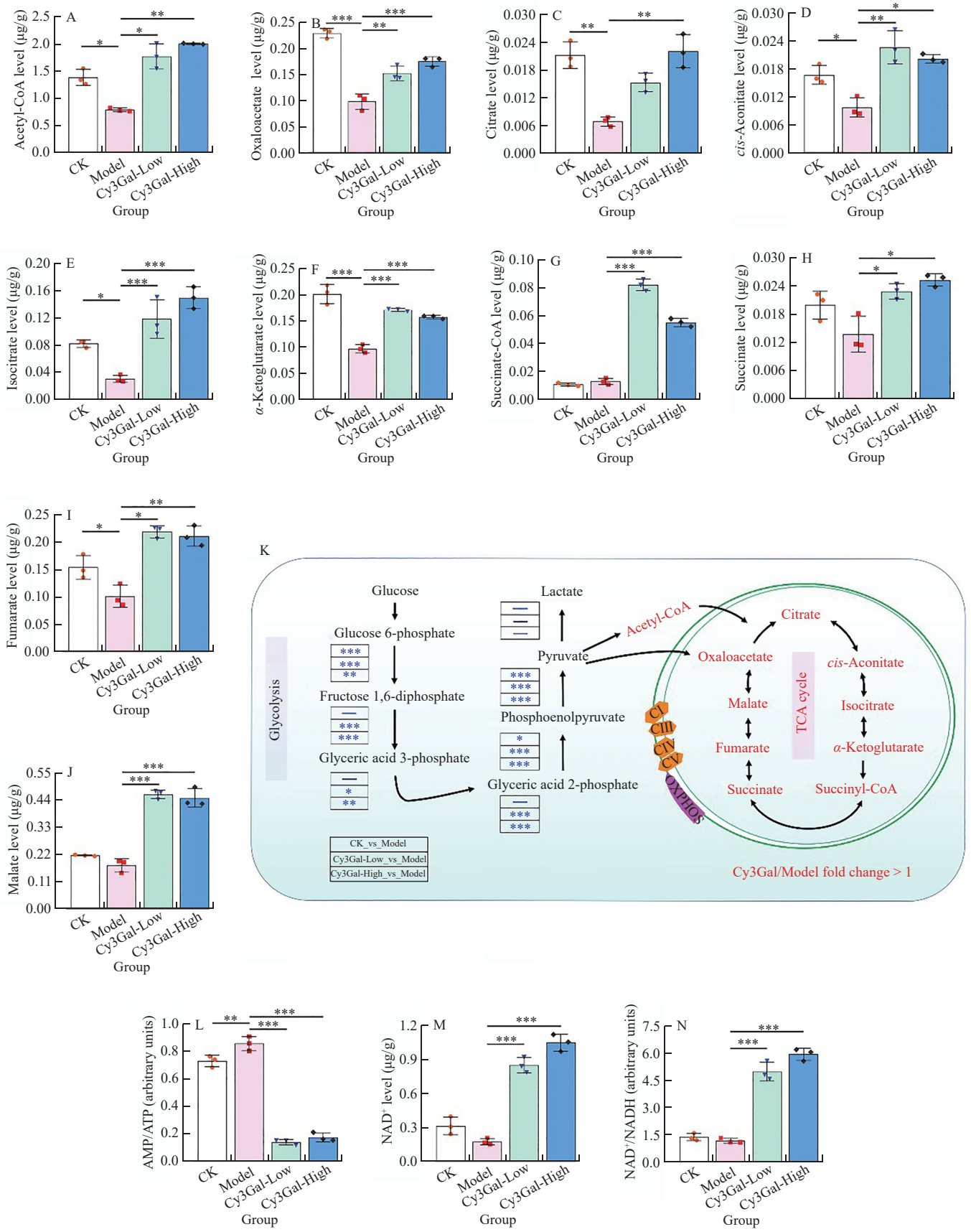


**Fig. 7** Cy3Gal enhanced TCA cycle metabolism in brain of overnourished mice ($n = 3$). (A-J) Levels of TCA circle related intermediates among different groups. (K) Cy3Gal increased glycolysis intermediates accumulation to augment TCA cycle metabolism in brain of overnourished mice. (L-M) $NAD^+$ levels and $NAD^+$/NADH ratios among different groups. (N) AMP/ATP ratios among different groups. $^*P < 0.05$, $^{**}P < 0.01$, $^{***}P < 0.001$, $^{-}P > 0.05$.

diet ($P < 0.001$, $P < 0.001$, respectively; Fig. 8). The increase of complex III activity might be a compensation mechanism acting simultaneously in OXPHOS[32], which indicated a huge demand for energy production in the HFHS-fed mice. Overall, Cy3Gal intervention improved complex I, IV, III, and V activities, which was conducive to enhancing mitochondrial respiration and energy production.

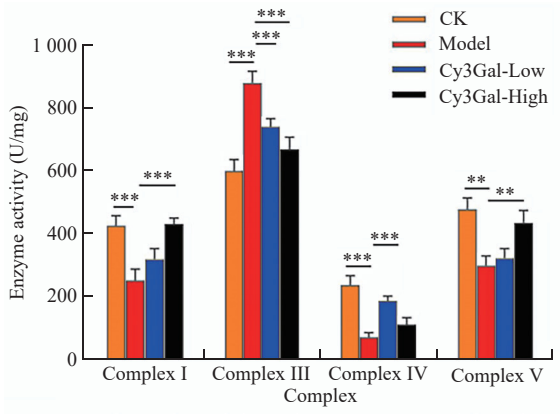


**Fig. 8** Cy3Gal regulated the activities of mitochondrial OXPHOS respiratory chain complex I, III, IV and V in brain of overnourished mice ($n = 3$). $^{**}P < 0.01$, $^{***}P < 0.001$.

## 4. Discussion

### *4.1 Cy3Gal promoted the blood glucose absorption and metabolism to provide a steady-state environment for brain energy supply*

T2DM may double the risk of dementia, and patients with T2DM are more susceptible to developing dementia at a younger age. In addition, the risk of cognitive decline will be increased even in the early stage of diabetes[33-34]. It has been observed that as the plasma glucose concentration continues to rise or fluctuate, the transport of glucose across the blood-brain barrier (BBB) is reduced to maintain a constant supply of glucose to the brain. The dysfunction of glucose transporting across the BBB or the decline in energy availability from OXPHOS result in insufficient glucose intake of neurons and low efficiency of brain energy acquisition[35]. Therefore, it is crucial to enhance the absorption and metabolism of high glucose concentration in the blood to effectively improve brain energy metabolism. In skeletal muscle of HFHS-diet fed mice, we observed the levels of glycolysis intermediates had strongly dietary effects, and Cy3Gal administration significantly increased the levels of the intermediates (Fig. 5A). We hypothesized that Cy3Gal converted the high concentration of blood glucose into lactate by enhancing glycolysis, thereby effectively improving the peripheral energy homeostasis in overnourished mice. The circulating lactate was likely to separate glycolysis from TCA cycle, and our analysis revealed that the levels of TCA cycle intermediates in skeletal muscle did not show major changes with Cy3Gal treatment (Fig. 5J). As a primary and universal carbohydrate energy source, circulating lactate enables significant glucose savings for crucial system activities (such as the brain and immune) and biochemical functions, which is conducive to effectively regulate the glucose utilization according to higher needs in body. Meanwhile, the increased lactate in brain has a positive impact on cognition[36], although Cy3Gal had little effect on lactate secretion in mice brain (Fig. 7K).

### *4.2 Cy3Gal improved glucose-derived metabolism in brain and promote neuron health*

The pyruvate dehydrogenase is active and TCA cycle activities are high in neurons, which makes neurons tend to perform OXPHOS in mitochondria to obtain 93% of bioenergy[37]. The analysis of glucose-derived intermediates revealed abnormal TCA cycle activity in the brain of HFHS diet-fed mice. Specifically, the levels of pyruvate, citrate, *cis*-aconitate, *α*-ketoglutarate, oxaloacetate, isocitrate, and fumarate were significantly decreased, while the levels of these intermediates were notably elevated with Cy3Gal treatment (Fig. 7). These intermediates play crucial roles in regulating TCA cycle activity, which in turn controls the concentrations of ATP and NADH, ensuring an adequate energy supply to the brain. The elevated $NAD^+$/NADH ratio suggested that Cy3Gal enhanced glucose metabolism in neurons (Fig. 7N)[38]. Besides, the increased levels of $NAD^+$, pyruvate, and oxaloacetate can also enhance TCA cycle activity, thereby improving the energy state in the mice brain. The consistent increases of $NAD^+$/NADH ratio induced by Cy3Gal in both skeletal muscle and brain could be attributed to its outstanding antioxidant properties and ability to improve antioxidant activities in neurons, which fortified neuroprotective effects. $NAD^+$ serves as a crucial coenzyme and cofactor in energy metabolism. The transformation reaction between $NAD^+$ and NADH can regulate activities of various dehydrogenases, and directly or indirectly affect metabolic pathways, cell aging, and other key cellular functions[39]. In our study, the decreased levels of *α*-ketoglutarate and the increased levels of isocitrate in skeletal muscle of Cy3Gal-treated mice might be related to the high $NAD^+$/NADH ratio. Moreover, many important cellular processes and functions for maintaining metabolic homeostasis and healthy aging are $NAD^+$-dependent, and the declined level of $NAD^+$ has a causal relationship with cognitive decline and metabolic diseases[40]. In the current study, we observed that Cy3Gal exerted profound efficacies to alleviate the neuron loss and improve cognitive impairment in overnourished mice (Figs. 2-4). Furthermore, mitochondrial OXPHOS function was found to be robust with the increased level of $NAD^+$ in brain, which protects against neuron loss and preserves cognition function of diabetes rats[41]. Meanwhile, the results indicated that the activities of mitochondrial respiratory chain complexes in brain were regulated by Cy3Gal under the HFHS feeding condition (Fig. 8).

### *4.3 Cy3Gal fortified mitochondrial respiration to maintain synaptic function and cognition*

Impaired glycolysis and TCA cycle can adversely affect axonal transport, mitochondrial function, and ATP production. Synaptic abnormalities and dysfunction caused by synaptic damage, synaptic loss, and synaptic structural changes often occur before the onset of behavioral symptoms[42]. Recently, researchers have developed modified therapies to prevent synaptic loss, strengthen synaptic connections, and increase synaptic density in order to rescue synaptic dysfunction and potentially prevent cognitive impairment[43]. Presynaptic local energy metabolism plays an important role in maintaining nerve conduction function, and the major presynaptic energy demand is powered by OXPHOS[44]. The expressions of Syn and PSD 95 in the hippocampus of mice were

severely disturbed under HFHS-diet feeding. However, Cy3Gal intervention increased synaptic density (Fig. 4), suggesting optimization of synaptic plasticity. Additionally, we found that Cy3Gal significantly reduced the AMP/ATP ratio (Fig. 7N), which was vital for supporting high-intensity synaptic activity and promoting synaptic energy balance. It was previously demonstrated that excessive accumulation of $\beta$-amyloid in brain led to neuron damage, disruption of synaptic plasticity, and mitochondrial dysfunction, further causing cognitive deficits[27]. However, our results supported that the aggregation and deposition of $\beta$-amyloid in brain may not be an essential factor for cognitive impairment, but rather a pathological symptom in the development of neurological diseases driven by energy metabolism disorders. Impairments in synapses and neurons could potentially arise as downstream consequences of compromised brain energy metabolism[45]. Finally, we revealed that Cy3Gal focalized the activation of mitochondrial respiration (Fig. 8), which is beneficial for maintaining synaptic plasticity. However, the specific underlying mechanisms need further study.

In summary, we have identified a promising dietary strategy to combat cognitive impairment and maintain brain health under the challenge of HFHS diet and the associated glucose metabolism disorder. Additionally, we have proposed a methodology to investigate the neuroprotective effects of dietary components by examining peripheral and brain bioenergetics.

## Conflict of interest

The authors declare that they have no known competing financial interests or personal relationships that could have appeared to influence the work reported in this paper.

## Acknowledgements

This work was supported by the National Natural Science Foundation of China (32172210).

## Appendix A. Supplementary information

Supplementary data associated with this article can be found, in the online version, at http://doi.org/10.26599/FSHW.2024.9250275.

## Data availability statement

The data that support the findings of this study are available from the corresponding author upon reasonable request.

### References

[1] F. Nazam, S. Shaikh, N. Nazam, et al., Mechanistic insights into the pathogenesis of neurodegenerative diseases: towards the development of effective therapy, Mol. Cell. Biochem. 476 (2021) 2739-2752. https://doi.org/10.1007/s11010-021-04120-6.

[2] F. Agosta, S. Galantucci, M. Filippi, Advanced magnetic resonance imaging of neurodegenerative diseases, Neurol. Sci. 38 (2017) 41-51. https://doi.org/10.1007/s10072-016-2764-x.

[3] P. Li, D. Feng, D. Yang, et al., Protective effects of anthocyanins on neurodegenerative diseases, Trends Food Sci. Tech. 117 (2021) 205-217. https://doi.org/10.1016/j.tifs.2021.05.005.

[4] G. Livingston, J. Huntley, A. Sommerlad, et al., Dementia prevention, intervention, and care: 2020 report of the Lancet Commission, Lancet 396 (2020) 413-446. https://doi.org/10.1016/S0140-6736(20)30367-6.

[5] L. Zhang, C. Chen, M.S. Mak, et al., Advance of sporadic Alzheimer's disease animal models, Med. Res. Rev. 40 (2020) 431-458. https://doi.org/10.1002/med.21624.

[6] J. Liu, T. Ye, Y. Zhang, et al., Protective effect of ginkgolide B against cognitive impairment in mice via regulation of gut microbiota, J. Agr. Food Chem. 69 (2021) 12230-12240. https://doi.org/10.1021/acs.jafc.1c05038.

[7] Z. H. Zhang, L. Wen, Q.Y. Wu, et al., Long-term dietary supplementation with selenium-enriched yeast improves cognitive impairment, reverses synaptic deficits, and mitigates tau pathology in a triple transgenic mouse model of Alzheimer's disease, J. Agr. Food Chem. 65 (2017) 4970-4979. https://doi.org/10.1021/acs.jafc.7b01465.

[8] K.G. Yiannopoulou, A.I. Anastasiou, V. Zachariou, et al., Reasons for failed trials of disease-modifying treatments for Alzheimer disease and their contribution in recent research, Biomedicines 7 (2019) 97. https://doi.org/10.3390/biomedicines7040097.

[9] S. Camandola, M.P. Mattson, Brain metabolism in health, aging, and neurodegeneration, EMBO J. 36 (2017) 1474-1492. https://doi.org/10.15252/embj.201695810.

[10] S.C. Cunnane, E. Trushina, C. Morland, et al., Brain energy rescue: an emerging therapeutic concept for neurodegenerative disorders of ageing, Nat. Rev. Drug Discov. 19 (2020) 609-633. https://doi.org/10.1038/s41573-020-0072-x.

[11] P. Mergenthaler, U. Lindauer, G.A. Dienel, et al., Sugar for the brain: the role of glucose in physiological and pathological brain function, Trends Neurosci. 36 (2013) 587-597. https://doi.org/10.1016/j.tins.2013.07.001.

[12] F. Yin, H. Sancheti, I. Patil, et al., Energy metabolism and inflammation in brain aging and Alzheimer's disease, Free Radical Bio. Med. 100 (2016) 108-122. https://doi.org/10.1016/j.freeradbiomed.2016.04.200.

[13] G.J. Biessels, F. Nobili, C.E. Teunissen, et al., Understanding multifactorial brain changes in type 2 diabetes: a biomarker perspective, Lancet Neurol. 19 (2020) 699-710. https://doi.org/10.1016/S1474-4422(20)30139-3.

[14] V. Srikanth, A.J. Sinclair, F. Hill-Briggs, et al., Type 2 diabetes and cognitive dysfunction-towards effective management of both comorbidities, Lancet Diabetes Endo. 8 (2020) 535-545. https://doi. org/10.1016/S2213-8587(20)30118-2.

[15] X. Zhang, T. Tong, A. Chang, et al., Midlife lipid and glucose levels are associated with Alzheimer's disease, Alzheimers Dement. 19 (2023) 181-193. https://doi.org/10.1002/alz.12641.

[16] Y. Mi, G. Qi, R. Fan, et al., EGCG ameliorates high-fat- and high-fructose-induced cognitive defects by regulating the IRS/AKT and ERK/CREB/BDNF signaling pathways in the CNS, FASEB J. 31 (2017) 4998-5011. https://doi.org/10.1096/fj.201700400RR.

[17] A. Mulati, S. Ma, H. Zhang, et al., Sea-buckthorn flavonoids alleviate high-fat and high-fructose diet-induced cognitive impairment by inhibiting insulin resistance and neuroinflammation, J. Agr. Food Chem. 68 (2020) 5835-5846. https://doi.org/10.1021/acs.jafc.0c00876.

[18] Z. Fan, H. Wen, X. Zhang, et al., Cyanidin 3-*O*-$\beta$-galactoside alleviated cognitive impairment in mice by regulating brain energy metabolism during aging, J. Agr. Food Chem. 70 (2022) 1111-1121. https://doi.org/10.1021/acs.jafc.1c06240.

[19] H. Wen, H. Cui, H. Tian, et al., Isolation of neuroprotective anthocyanins from black chokeberry (*Aronia melanocarpa*) against amyloid-beta-induced cognitive impairment, Foods 10 (2020) 63. https://doi.org/10.3390/foods10010063.

[20] L. Liang, G. Liu, G. Yu, et al., Urinary metabolomics analysis reveals the anti-diabetic effect of stachyose in high-fat diet/streptozotocin-induced type 2 diabetic rats, Carbohyd. Polym. 229 (2020) 115534. https://doi. org/10.1016/j.carbpol.2019.115534.

[21] M. Hahn, P.P. van Krieken, C. Nord, et al., Topologically selective islet vulnerability and self-sustained downregulation of markers for beta-cell maturity in streptozotocin-induced diabetes, Commun. Biol. 3 (2020) 541. https://doi.org/10.1038/s42003-020-01243-2.

[22] S. Suzuki, S. Aoe, High $\beta$-glucan barley supplementation improves glucose tolerance by increasing GLP-1 secretion in diet-induced obesity mice, Nutrients 13 (2021) 527. https://doi.org/10.3390/nu13020527.

[23] M. van de Wouw, A.M. Walsh, F. Crispie, et al., Distinct actions of the fermented beverage kefir on host behaviour, immunity and microbiome gut-

brain modules in the mouse, Microbiome 8 (2020) 67. https://doi.org/10.1186/s40168-020-00846-5.

[24] S.P.L. Dos, P.F. Ozela, D.B.B.M. de Fatima, et al., Alzheimer's disease: a review from the pathophysiology to diagnosis, new perspectives for pharmacological treatment, Curr. Med. Chem. 25 (2018) 3141-3159. https://doi.org/10.2174/0929867323666161213101126.

[25] R. Schurr, A.A. Mezer, The glial framework reveals white matter fiber architecture in human and primate brains, Science 374 (2021) 762-767. https://doi.org/10.1126/science.abj7960.

[26] V.T. Chou, S.A. Johnson, D. van Vactor, Synapse development and maturation at the drosophila neuromuscular junction, Neural Dev. 15 (2020) 11. https://doi.org/10.1186/s13064-020-00147-5.

[27] S. Li, Z.H. Sheng, Energy matters: presynaptic metabolism and the maintenance of synaptic transmission, Nat. Rev. Neurosci. 23 (2022) 4-22. https://doi.org/10.1038/s41583-021-00535-8.

[28] Y. Liu, H. Liu, J. Yang, et al., Increased amyloid beta-peptide (1-40) level in brain of streptozotocin-induced diabetic rats, Neuroscience 153 (2008) 796-802. https://doi.org/10.1016/j.neuroscience.2008.03.019.

[29] N.J. Bryant, G.W. Gould, Insulin stimulated GLUT4 translocation-size is not everything! Curr. Opin. Cell Biol. 65 (2020) 28-34. https://doi.org/10.1016/j.ceb.2020.02.006.

[30] M.P. Bordone, M.M. Salman, H.E. Titus, et al., The energetic brain-a review from students to students, J. Neurochem. 151 (2019) 139-165. https://doi.org/10.1111/jnc.14829.

[31] J. Gu, M. Wu, R. Guo, et al., The architecture of the mammalian respirasome, Nature 537 (2016) 639-643. https://doi.org/10.1038/nature19359.

[32] Z. Fisar, H. Hansikova, J. Krizova, et al., Activities of mitochondrial respiratory chain complexes in platelets of patients with Alzheimer's disease and depressive disorder, Mitochondrion 48 (2019) 67-77. https://doi.org/10.1016/j.mito.2019.07.013.

[33] A. Ott, R.P. Stolk, F. van Harskamp, et al., Diabetes mellitus and the risk of dementia: The Rotterdam Study, Neurology 53 (1999) 1937-42. https://doi.org/10.1212/wnl.53.9.1937.

[34] E.E. Sundermann, K.R. Thomas, K.J. Bangen, et al., Prediabetes is associated with brain hypometabolism and cognitive decline in a sex-dependent manner: a longitudinal study of nondemented older adults, Front. Neurol. 12 (2021) 551975. https://doi.org/10.3389/fneur.2021.551975.

[35] E.K. Wardzinski, A. Kistenmacher, U.H. Melchert, et al., Impaired brain energy gain upon a glucose load in obesity, Metabolism 85 (2018) 90-96. https://doi.org/10.1016/j.metabol.2018.02.013.

[36] H.L. El, M. Khalifeh, V. Zibara, et al., Lactate mediates the effects of exercise on learning and memory through SIRT1-dependent activation of hippocampal brain-derived neurotrophic factor (BDNF), J. Neurosci. 39 (2019) 2369-2382. https://doi.org/10.1523/JNEUROSCI.1661-18.2019.

[37] G. Yellen, Fueling thought: management of glycolysis and oxidative phosphorylation in neuronal metabolism, J. Cell Biol. 217 (2018) 2235-2246. https://doi.org/10.1083/jcb.201803152.

[38] S. Mason, Lactate shuttles in neuroenergetics-homeostasis, allostasis and beyond, Front. Neurosci. 11 (2017) 43. https://doi.org/10.3389/fnins.2017.00043.

[39] S. Sahar, V. Nin, M.T. Barbosa, et al., Altered behavioral and metabolic circadian rhythms in mice with disrupted $NAD^+$ oscillation, Aging (Albany NY) 3 (2011) 794-802. https://doi.org/10.18632/aging.100368.

[40] A.J. Covarrubias, R. Perrone, A. Grozio, et al., $NAD^+$ metabolism and its roles in cellular processes during ageing, Nat. Rev. Mol. Cell Bio. 22 (2021) 119-141. https://doi.org/10.1038/s41580-020-00313-x.

[41] K. Chandrasekaran, J. Choi, M.I. Arvas, et al., Nicotinamide mononucleotide administration prevents experimental diabetes-induced cognitive impairment and loss of hippocampal neurons, Int. J. Mol. Sci. 21 (2020) 3756. https://doi.org/10.3390/ijms21113756.

[42] J. Jackson, E. Jambrina, J. Li, et al., Targeting the synapse in Alzheimer's disease, Front Neurosci. 13 (2019) 735. https://doi.org/10.3389/fnins.2019.00735.

[43] L. Peng, I. Bestard-Lorigados, W. Song, The synapse as a treatment avenue for Alzheimer's disease, Mol. Psychiatr. 27 (2022) 2940-2949. https://doi.org/10.1038/s41380-022-01565-z.

[44] D. Attwell, S.B. Laughlin, an energy budget for signaling in the grey matter of the brain, J. Cerebr. Blood F. Met. 21 (2001) 1133-1145. https://doi.org/10.1097/00004647-200110000-00001.

[45] E. Jamasbi, J.D. Wade, F. Separovic, et al., Amyloid beta (Aβ) peptide and factors that play important roles in Alzheimer's disease, Curr. Med. Chem. 23 (2016) 884-892. https://doi.org/10.2174/0929867323666160229113911.